論文 97-22-3-1

Pattern Spectrum Component Function and Warning Traffic Sign Recognition

Heo Jin Kim*, Gang Yi Jiang**, Tae Young Choi*** *Regular Members*

패턴 스펙트럼 성분 함수와 주의 교통 표지 인식

正會員 김 회 진*, 장 강 의**, 최 태 영***

ABSTRACT

In this paper, a pattern spectrum component function is introduced for an oriented shape analysis and its properties are discussed. It can represent directional information of shape more precisely than the conventional oriented pattern spectrum. An adaptive distance function between two pattern spectrum component functions is presented to recognize different shapes in noise. As a practical application, the pattern spectrum component function is applied to warning traffic sign recognitions utilizing the adaptive distance functions. Favorable results are obtained compared to the oriented pattern spectrum.

요 약

기존의 방향성 패턴 스펙트럼에 비하여 보다 정확하게 방향성 정보를 나타낼 수 있는 패턴 스펙트럼 성분 함수를 도입하고 그 성질을 분석하였다. 그리고 패턴 스펙트럼 성분 함수에 의하여 잡음성 형상을 식별하고자 적응 거리 함수를 제안하였다. 제안한 패턴 스펙트럼 성분 함수를 주의 교통 표지 식별에 실제 응용하여 적응 거리 함수에 의하여 평가한 본 결과 방향성 패턴 스펙트럼에 비하여 보다 만족할 만한 결과를 얻을 수 있었다.

I. Introduction

The shape representation and shape-size description are very important in image processing and computer vision [1]. Mathematical morphology provides an efficient approach to description and analysis of shapes [2-4]. In recent decade, many methods for shape analysis based on the mathematical morphology have been proposed [5-10], which can be classified into two categories: shape structure enhancement and quantitative

*Dept. of Electronics, Dongmyung Junior College
** Dept. of Electronics Engineering, Hangzhou University, P. R. China
*** School of Electrical and Electronics Engineering, Ajou University
論文番號:96054-0209
接受日字:1996年 2月 9日

shape description. The pattern spectrum, also called a morphological shape-size histogram, is an important tool for shape representation in morphological image analysis [3, 6]. It is a quantitative description of shape, derived from the morphological size distribution (also called "granulometeries" in [2, 10]).

In recent researches, Goustias proposed a generalized form of pattern spectrum for multi-structuring elements [7], Shih a geometric spectrum based on the morphological skeleton transformation [11], Regazzoni a statistical pattern spectrum [12], and Zhou a high order pattern spectrum [13]. However, an oriented information of shape has not been respected in these researches because the employed structuring elements (SEs) such as octagon, square and rhombus are not adequate to linear directional shapes.

In this paper, the pattern spectrum component function is introduced to represent a directional information which is difficult to be described by the formal pattern spectrum. And its properties are discussed.

Ⅱ. Pattern Spectrum and Oriented Pattern Spectrum

2.1 Pattern Spectrum

Let I be a compact continuous binary image, and let B be a continuous binary pattern, called the SE. Then, the basic morphological operations are represented as follows

$$\text{dilation}: I \oplus B = \{a ; \hat{B}_a \cap I \neq \Phi\},$$
$$\text{erosion}: I \ominus B = \{a ; B_a \subseteq I\}$$
$$\text{opening}: I \circ B = (I \ominus B) \oplus B,$$
$$\text{closing}: I \bullet B = (I \oplus B) \ominus B,$$

where $\hat{B} = \{-b ; b \in B\}$ and B_a is the translated B by a.

Then, the pattern spectrum of I with respect to B is given as follows [6]

$$PS(I, B, r) = \begin{cases} -\dfrac{dA(I \circ rB)}{dr}, & r \geq 0 \\ -\dfrac{dA(I \bullet rB)}{dr}, & r < 0 \end{cases} \quad (1)$$

where A(I) denotes the area of I and $rB = \{rb ; b \in B\}$.

The pattern spectrum can describe the following informations of shape I :

1. The lower size parts of the pattern spectrum represent boundary roughness in I relative to B.
2. The isolated impulses in the pattern spectrum illustrate long capes or bulky protruding parts in I.

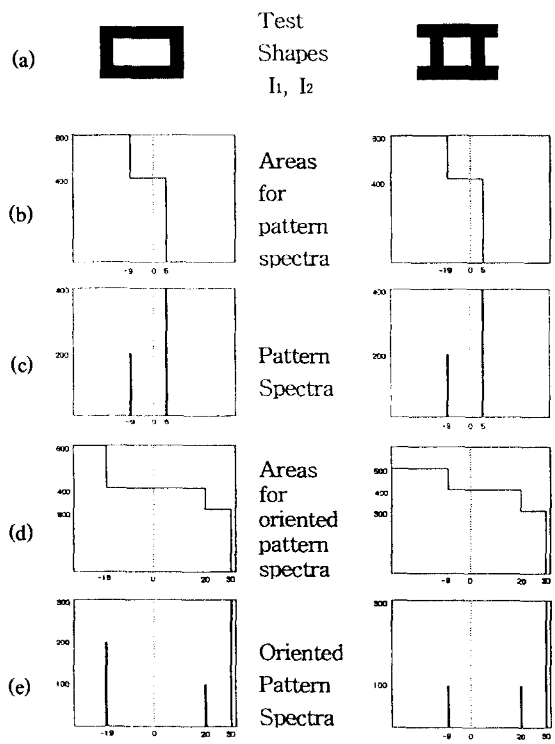

Fig. 1 Examples of pattern spectra and oriented pattern spectra. (a) Two test images Ii (i = 1, 2) similar to Korean consonants of ㅁ and ㅍ, with the same areas and widths of 400 and 5, respectively, (b) Area functions of Ii rB for $r \geq 0$ and $Ii \bullet rB$ for $r < 0$, (c) Pattern spectra of PS(Ii, B, r), (d) Area functions of $\bigcup_\theta (Ii \circ rL_\theta)$ for $r \geq 0$ and $\bigcap_\theta (Ii \bullet rL_\theta)$ for $r < 0$, (d) Oriented pattern spectra of OPS(Ii, r).

3. PS(I, B, r)/A(I) represents the maximal degree that I contains the pattern rB.
4. The big impulses at negative r illustrate the existence of prominent intruding gulfs and holes in I.

However, in most applications of the pattern spectrum, the typical binary area shapes, such as circle, square, and rhombus, are chosen as the SEs. Fig.1(a), (b) and (c) show examples of pattern spectrum using a 3×3 square SE, where we have used two shapes of Korean consonant styles such as ㅁ and ㅍ with the same width of 5 within 20×30 rectangle. We see that they have the same pattern spectra and thus it is impossible to discern between them.

2.2 Oriented Pattern Spectrum

To enable the pattern spectrum to extract directional informations of shape, Maragos proposed an oriented pattern spectrum, denoted OPS(I, r), as follows [6].

$$\mathrm{OPS}(I, r)=\begin{cases} -\dfrac{dA(\bigcup_{\theta}(I \circ rL_{\theta}))}{dr}, & r\geq 0 \\ -\dfrac{dA(\bigcap_{\theta}(I \bullet rL_{\theta}))}{dr}, & r<0 \end{cases} \qquad (2)$$

where L_{θ} denotes an unit-length line segment SE passing through the origin and forming an angle θ with the horizontal $(0\leq\theta\leq 2\pi)$.

Fig. 1(d) and (e) show the results of oriented pattern spectra corresponding to Fig. 1(a), where we have used four directional line segment SEs: 0°{(0, 0)−(1, 0)}, 45°{(0, 0)−(1, 1)}, 90°{(0, 0)−(0, 1)}, 135°{(0, 0)−(−1, 1)}. The result indicates that two shapes consist of line segments of the same lengths of 20 and 30, and that they have rectangular holes of 20×10 and 10×10, respectively. But it does not inform about any oriented angle. The union and intersection operations over θ in Eq. (2) give rise to lose each directional information.

Ⅲ. Pattern Spectrum Component Function

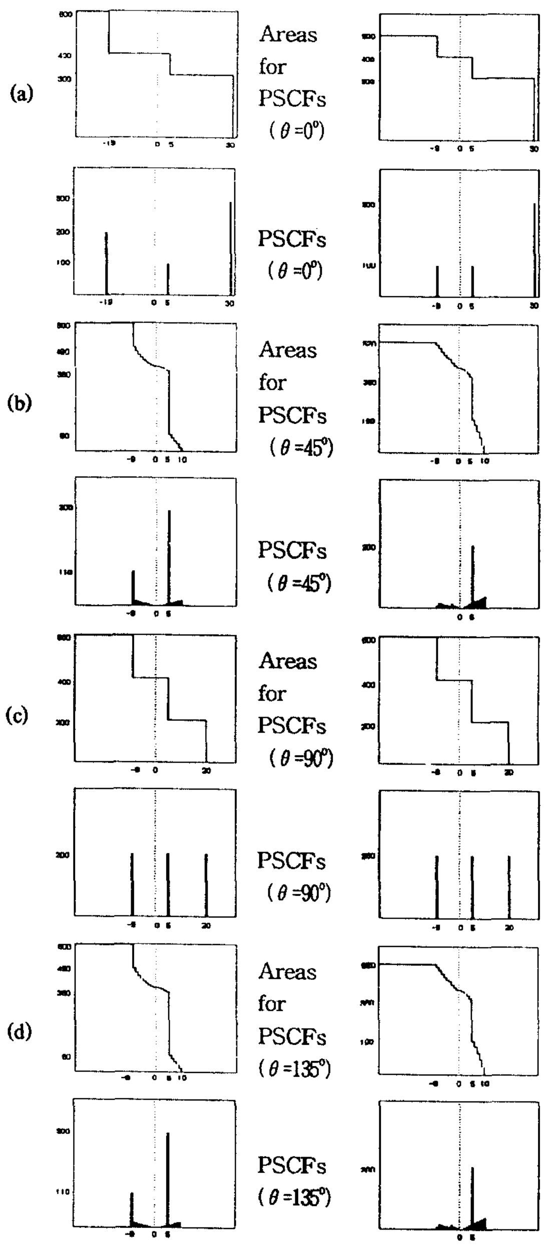

Fig. 2 PSCFs for $\theta=0°$, 45°, 90°, 135° of Fig. 1(a). (a) The upper left and right graphs represent area functions of $I_i \circ rL_{\theta}$ for $r\geq 0$ and $I_i \bullet rL_{\theta}$ for $r<0$ when $\theta=0°$, corresponding to ㅁ and ㅍ of Fig. 1(a), respectively, and the lower are their PSCFs. In this manner, the area functions and PSCFs for $\theta=45°$, 90°, and 135° are depicted in (b), (c), and (d), respectively.

To alleviate the problem of losing directional informations, we adopt a new approach to keeping θ in Eq. (2) alive. We define a function, called a pattern spectrum component function (PSCF), denoted PSC (I, θ, r), as

$$PSC(I, \theta, r)=\begin{cases} -\dfrac{-dA(I \circ rL_\theta)}{dr}, & r \geq 0 \\ -\dfrac{-dA(I \bullet rL_\theta)}{dr}, & r<0 \end{cases} \tag{3}$$

which can be also considered as a special type of pattern spectrum by adopting a line segment SE L_θ instead of area SE B in Eq. (1).

Fig. 2 shows the results of PSCFs using the same four L_θ's ($\theta=0°$, $45°$, $90°$, $135°$) as used in the oriented pattern spectrum in Fig. 1(d). We see that the four PSCFs are much different with θ and that the PSCFs of two shapes ㅁ and ㅍ are distinguishable for the cases of $\theta=0°$, $45°$ and $135°$ except for $\theta=90°$.

3.1 Properties of PSCF

1. Non-negative.

   Each element of PSCF is positive:

   $PSC(I, \theta, r) \geq 0$ for $\forall r$ and $\forall \theta$.

2. Energy identity.

   The sum of PSCF of a shape at any direction θ equals to the total area of the shape:

   $\int_0^\infty PSC(I, \theta, r)\, dr = A(I)$ for $\forall \theta$.

3. Translation invariance.

   The PSCF is translation invariant on I:

   $PSC(I_d, \theta, r)=PSC(I, \theta, r)$ for $d \in R^2$

4. Rotation properties.

   ① $PSC(Rot(I, \alpha), \theta, r)=PS(I, \theta+\alpha, r)$,

   where $Rot(I, \alpha)$ expresses the counterclockwise rotated I by an angle α.

   ② $\int_{-\pi}^{\pi} PSC(Rot(I, \alpha), \theta, r)\, d\theta=\int_{-\pi}^{\pi} PSC(I, \theta, r)\, d\theta$

5. Periodicity.

   The PSCF is a periodic function with respect to θ with a period of π:

   $PSC(I, \pi+\theta, r)=PSC(I, \theta, r)$.

6. Symmetries.

   ① If I is symmetric on the direction α, its PSCF is symmetric on the direction α, too.

   ② If I is symmetric with J on the direction α, then

   $PSC(J, \theta, r)=PSC(I, 2\alpha-\theta, r)$.

7. Additivity.

   For a mutually exclusive set, i.e., if $I=I_1 \cup I_2 \cup \ldots \cup I_N$ and $I_i \cap I_j=\Phi$ for $i \neq j$, then

   $PSC(I, \theta, r)=\sum_n PSC(I_n, \theta, r)$ for $r \geq 0$.

3.2 PSCF of Discrete Binary Image

Let X be a finite-extent discrete binary image. Then, its PSCF at discrete θ can be similarly obtained from Eq. (3) by exchanging the differential area and the real number r by the difference of cardinality and an integer n, respectively, as

$$PSC(X, \theta, n)=\begin{cases} Card(X \circ nL_\theta \backslash X \circ (n+1)L_\theta), & n \geq 0 \\ Card(X \bullet (-n)L_\theta \backslash X \bullet (-1-n)L_\theta), & n<0 \end{cases} \tag{4}$$

where Card(X) denotes the cardinality (the total number of elements) of X, $\backslash$ set difference, and nL_θ the origin set $\{o\}$ dilated by L_θ n times, i.e.,

$nL_\theta=(\cdots((\{o\} \oplus L_\theta) \oplus L_\theta)\cdots) \oplus L_\theta$. Note that $0L_\theta=\{o\}$.

The PSCF of X at any angle θ is, similarly as stated in rotation property, equal to that of $Rot(X, \theta)$ at zero angle. We can thus rewrite Eq. (4) as follows.

$$PSC(X, \theta, n)=\begin{cases} Card(Rot(X, \theta) \circ nL_0 \backslash Rot(X, \theta) \\ \quad \circ (n+1)L_0), & n \geq 0 \\ Card(Rot(X, \theta) \bullet (-n)L_0 \backslash Rot(X, \theta) \\ \quad \bullet (-1-n-L_0), & n<0 \end{cases}$$

3.3 Adaptive Distance Function

For comparison of two PSCFs, we adopt a distance function based on mean square error as

$$D(X, Y) = \sqrt{\sum_{\theta} w(\theta) \sum_{n} (PSC(X, \theta, n) - PSC(Y, \theta, n))^2} \quad (5)$$

where $w(\theta)$ is a positive weighting factor with $\sum_{\theta} w(\theta) = 1$. As the distance is smaller, the shape X resembles Y more closely.

In consideration of noisy shapes, we develop an adaptive algorithm to be robust to scale changes modifying Eq. (5) as follows

Adaptive Distance Function

For each θ, do:
{ for each n, compute
$T = \min_{m} \{(PSC(X, \theta, n) - PSC(Y, \theta, m))^2;$
$\leq |m-n| \leq N_l\};$
$d(\theta) = d(\theta) + T;$
mark $PSC(Y, \theta, m')$ as visited,
which corresponds to T.
for each m'' not visited, compute
$d(\theta) = d(\theta) + \min_{k} \{(PSC(Y, \theta, m'') - PSC(X, \theta, k))^2;$
$|m''-k| \leq N_l\};$ }
Finally, adaptive distance

$$D_a(X, Y) = \sqrt{\sum_{\theta} w(\theta) d(\theta)} \quad (6)$$

Note that the search interval N_l in the adaptive distance function is assumed to be very small positive integer, for example, $N_l = 1$ or 2, and that this adaptive distance function is not commutative, i.e., $D_a(X, Y) \neq D_a(Y, X)$.

We can use the adaptive distance function for the pattern spectrum PS( ) in Eq. (1) and the oriented spectrum OPS( ) in Eq. (2) by exchanging the differential area and the real number r for the difference of cardinality and an integer n, respectively. Of course, in the adaptive distance function, it requires only one repetition process with respect to θ, since θ is not variable but fixed.

Ⅳ. Experimental Results

To test performances of shape recognitions using the pattern spectrum PS( ) in Eq. (1), the oriented spectrum OPS( ) in Eq. (2), and pattern spectrum component function PSC( ) in Eq. (3), simulations are carried out for recognition of 22 symbols in the Korean warning traffic signs on road.

Fig. 3 shows 22 reference symbols (Xi's) and filtered noisy symbols (Yi's), which are first corrupted by 10% salt and pepper noise and then filtered by morphological open-close operation using 3×3 square SE.

With the reference symbols and noisy symbols in Fig. 3, respectively denoted by Xi and Yi, we have computed adaptive distances $D_a(Y_i, X_j)$ in Eq. (6) (i, j = 1, 2, ⋯, 22).

Table 1 shows adaptive distances $D_a(Y_i, X_j$ in Eq. (6) using pattern spectrum component functions in Eq. (3) with $\theta = 0°$, 45°, 90°, and 135°. Here we consider Y_i as X_k when the k-th element is the smallest, which is marked by underline, among all elements of the i-th row. In Table 1, there are four symbols mistaken by others: Y_5 as X_8, Y_{16} as X_{15}, Y_{17} as X_{15}, and Y_{21} as X_{20}. We can interpret these errors by rotation invariant property of pattern spectrum component functions as noted in section 3.1 since X_5 and X_{21} are rotated X_4 and X_{20} by an angle 180o, respectively, and both X_{16} and X_{17} are in some degree similar to X_{15} in directional pattern spectrum components of $\theta = 45°$, 90°, and 135°.

Similarly Table 2 and 3 show adaptive distances using oriented pattern spectra in Eq. (2) with $\theta = 0°$, 45°, 90°, and 135°, and using pattern spectra in Eq. (1) with 3×3 square SE, respectively. There are, in Table 2 and 3, nine and sixteen symbols mistaken by others, respectively.

With these failure rates of recognitions, the proposed pattern spectrum component function shows the best performance, while the pattern spectrum is the

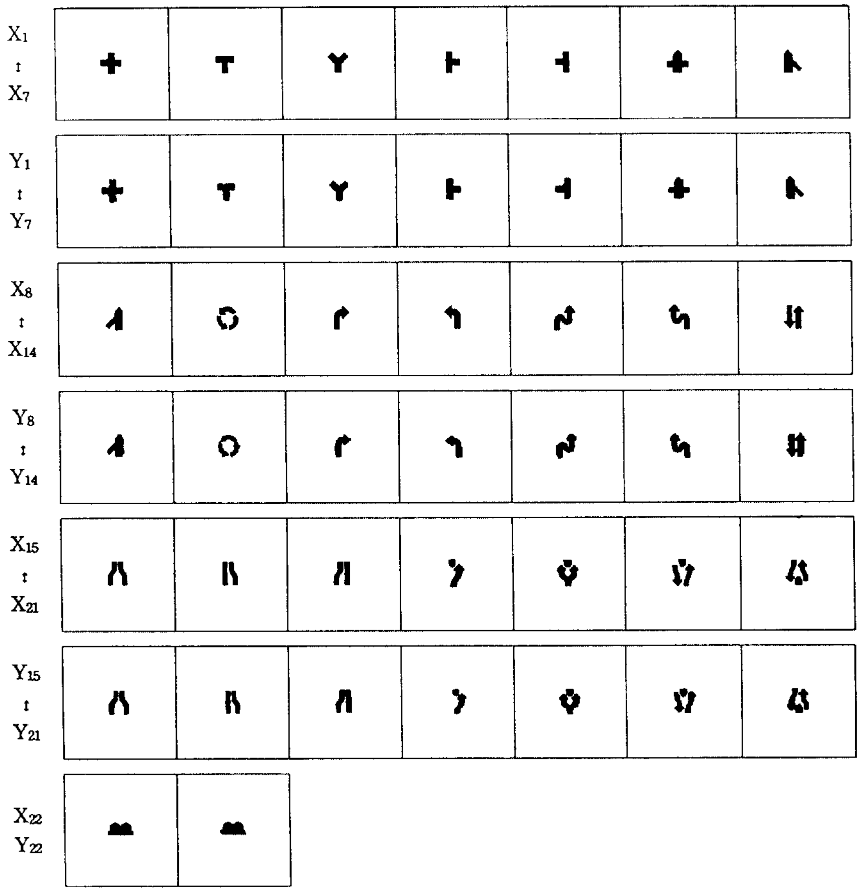

Fig. 3 Reference symbols (X_i) and their filtered noisy symbols (Y_i) for i = 1~22.

worst.

In fact two shapes rotated by an angle 180°, each spectrum results in the same result. But as we see in Table 1, 2, and 3, it is not so. This tells us that the above three algorithms are not much robust to noise. This may be improved by normalizing T by n in adaptive distance function since it can reduce the noisy effect for long capes or long holes.

Ⅴ. Conclusions

In this paper, the PSCF is introduced and its properties are discussed. The PSCF can represent oriented informations of the shape, and is more suitable to describe the shape of object than both the oriented pattern spectrum and the pattern spectrum. And with the proposed adaptive distance function, the PSCF can recognize 18 warning symbols among 22 in noise. The PSCF may be very attractive to analysis of the other traffic signs, especially, indicatory signs, since all of them consist of directional shapes. However rotated symbols such as ← and →, ⊢ and ⊣, etc., and some symbols of equal directional components such as ← and →, ↗ and ↘, etc., can not be made a distinction between them.

Table 1. $D_a(X_i, X_j)$ using the pattern spectrum component functions.

Yi	Reference Symbols Xi (i = 1, 2, · · ·, 22)																					failure
	1	2	3	4	5	6	7	8	9	10	11	12	13	14	15	16	17	18	19	20	21	22	
1	118	162	264	300	307	318	291	295	374	356	354	395	399	680	608	690	741	288	362	424	453	406	0
2	249	169	273	337	345	324	285	311	356	258	261	303	298	591	574	673	658	295	344	356	429	387	0
3	343	342	149	377	387	387	355	373	366	321	323	342	342	657	539	644	711	267	305	406	406	392	0
4	269	224	318	146	154	448	256	257	392	328	335	421	436	679	592	680	751	299	366	431	442	439	0
5	309	267	324	311	317	397	301	287	382	383	389	435	445	695	617	704	768	362	419	456	477	436	x
6	368	375	368	476	483	101	274	286	425	424	421	426	431	733	643	721	789	440	454	498	555	408	0
7	450	420	437	484	491	324	90	265	411	413	427	394	394	714	615	704	762	452	506	492	541	463	0
8	434	411	395	479	486	353	308	138	441	431	423	385	403	732	609	698	778	444	502	506	527	451	0
9	415	378	335	415	424	450	391	411	124	305	297	300	322	595	390	491	629	312	315	262	293	424	0
10	353	271	245	238	248	455	363	382	370	145	178	257	244	480	533	646	543	221	296	312	394	449	0
11	348	270	275	235	241	483	307	315	372	288	217	338	321	538	598	690	644	301	352	382	430	466	0
12	386	309	281	392	399	448	389	384	350	251	264	177	198	513	444	571	580	269	337	246	322	422	0
13	404	319	298	398	406	476	400	416	353	242	270	196	183	518	435	559	584	274	319	284	325	433	0
14	555	469	550	412	413	700	644	659	607	388	377	376	362	175	636	727	357	444	520	381	490	705	0
15	546	467	422	492	500	604	541	540	340	314	307	264	258	486	189	370	458	305	322	249	232	498	x
16	613	591	504	625	632	644	588	594	376	362	343	345	299	306	178	181	327	481	454	383	289	598	x
17	656	523	544	419	421	694	639	659	531	384	394	407	391	288	186	206	223	374	475	406	316	655	0
18	307	256	234	327	337	429	374	388	293	198	246	227	246	524	387	534	540	190	266	226	282	417	0
19	413	364	313	395	400	509	448	438	377	354	345	388	378	556	458	553	611	284	153	326	354	391	0
20	500	371	402	424	430	586	478	477	334	254	282	242	262	439	312	454	468	231	318	146	157	576	0
21	477	362	367	399	406	527	449	452	326	249	242	228	235	463	317	446	503	250	286	129	183	541	x
22	458	462	390	528	536	428	471	473	463	438	444	449	462	763	581	709	770	458	411	557	549	176	0

Table 2. $D_a(X_i, X_j)$ using the oriented pattern spectra.

Yi	Reference Symbols Xi (i = 1, 2, · · ·, 22)																					failure
	1	2	3	4	5	6	7	8	9	10	11	12	13	14	15	16	17	18	19	20	21	22	
1	61	50	236	193	207	48	110	116	335	155	153	226	225	61	298	150	143	221	533	257	286	208	x
2	80	75	185	232	245	71	75	80	333	158	158	187	184	74	291	133	139	202	534	249	289	204	x
3	316	313	98	297	302	313	180	165	323	229	236	126	97	294	261	235	260	197	520	334	319	312	x
4	232	228	246	99	117	228	249	233	345	142	125	255	277	232	217	163	175	274	380	310	278	195	0
5	239	235	195	286	295	234	168	142	396	244	244	236	200	238	314	191	240	269	571	324	333	306	x
6	49	34	267	227	241	30	118	134	329	171	171	255	252	57	327	178	162	237	546	270	300	204	0
7	128	123	161	201	213	122	46	50	332	178	178	197	199	129	317	152	180	222	546	265	271	232	0
8	203	201	157	241	250	201	87	50	367	210	210	218	191	206	315	186	225	228	554	290	297	283	0
9	305	311	278	291	295	297	309	301	97	259	247	179	192	273	158	227	199	149	381	222	143	246	0
10	218	215	183	149	155	212	181	180	285	115	109	198	183	209	175	170	153	183	381	282	279	116	0
11	186	183	161	170	178	178	167	156	282	78	69	151	147	170	146	89	85	163	408	245	256	132	0
12	306	304	133	214	215	295	226	214	285	231	231	129	72	265	169	146	199	195	493	284	268	305	x
13	304	303	168	192	192	298	235	215	281	204	205	164	104	275	110	161	192	213	463	288	251	293	0
14	92	86	264	240	253	81	167	177	293	162	172	217	222	32	276	138	122	202	529	259	278	166	0
15	387	386	179	256	258	380	320	304	265	255	259	191	191	351	130	193	245	221	350	324	270	279	0
16	222	218	194	219	226	210	214	188	259	95	91	169	172	201	123	113	85	164	390	268	216	150	x
17	196	192	198	223	232	187	206	184	288	66	68	146	158	160	161	60	40	171	424	270	256	155	0
18	216	226	225	213	220	216	240	228	200	199	179	194	218	197	214	164	165	150	387	136	123	254	x
19	510	517	445	382	380	517	512	500	374	379	379	433	447	502	361	424	415	364	122	433	380	313	0
20	247	263	302	319	326	250	269	269	125	262	256	236	248	247	268	241	205	164	458	58	123	289	0
21	256	270	284	306	313	256	266	259	95	242	239	211	218	253	224	228	194	155	429	128	95	275	x
22	162	157	270	176	186	156	213	211	321	67	70	253	257	156	193	142	98	202	413	272	277	129	x

Table 3. $D_a(X_i, X_j)$ using the pattern spectra. The symbol +denotes a number of two ciphers, so that for example, 13+ is greater than 1300.

Yi	Reference Symbols Xi (i = 1, 2, · · ·, 22)																					failure
	1	2	3	4	5	6	7	8	9	10	11	12	13	14	15	16	17	18	19	20	21	22	
1	777	303	377	544	553	648	730	738	847	327	331	518	528	637	10+	11+	603	435	315	645	833	798	x
2	851	191	131	594	604	844	482	489	836	281	325	644	660	781	10+	11+	746	369	333	713	807	854	x
3	908	283	164	633	644	850	493	505	567	226	214	605	639	799	683	740	763	198	350	505	442	809	0
4	581	111	225	307	318	904	232	240	834	484	513	884	909	10+	961	10+	10+	349	569	816	723	904	x
5	803	354	265	545	555	485	434	440	857	604	616	959	984	11+	10+	10+	11+	463	704	898	814	626	x
6	11+	816	770	955	964	147	267	273	956	759	763	909	926	10+	11+	12+	10+	769	830	914	993	463	0
7	13+	966	885	11+	11+	394	50	52	862	860	856	10+	10+	12+	10+	10+	11+	824	997	955	901	376	0
8	13+	968	895	11+	11+	344	51	63	891	868	866	10+	10+	12+	10+	11+	12+	859	10+	973	926	419	x
9	14+	10+	655	11+	11+	11+	925	925	177	467	441	218	264	535	355	472	501	591	456	195	217	914	0
10	578	239	283	270	283	882	968	975	754	265	241	224	236	393	10+	10+	349	362	279	476	789	907	x
11	940	317	253	652	664	851	537	543	647	139	156	565	591	768	908	979	725	169	321	568	641	770	x
12	10+	461	271	574	583	894	976	982	269	206	223	422	448	645	491	585	607	174	203	246	324	928	x
13	11+	539	451	364	371	912	10+	10+	403	325	326	342	343	435	351	388	404	388	106	359	233	10+	x
14	921	446	434	419	438	904	11+	11+	570	357	328	307	340	599	633	655	537	446	236	179	481	10+	x
15	14+	914	596	886	895	10+	950	954	347	283	284	185	218	507	387	465	446	402	106	277	183	938	x
16	14+	10+	763	12+	12+	12+	997	998	393	460	437	103	95	281	80	215	246	704	392	390	242	993	x
17	14+	903	670	370	376	977	10+	10+	342	418	397	93	130	387	181	332	356	558	436	362	215	10+	x
18	12+	724	497	705	717	913	822	827	233	117	133	438	479	738	611	684	683	149	320	350	350	774	x
19	776	188	123	542	550	874	991	10+	531	225	238	263	328	597	751	800	542	290	108	143	534	945	0
20	14+	914	619	709	716	10+	10+	10+	263	327	297	326	367	654	428	550	588	487	211	94	263	10+	0
21	12+	766	426	914	924	10+	937	938	285	223	207	278	303	550	428	504	496	370	197	345	215	920	x
22	14+	10+	10+	12+	12+	342	11+	11+	10+	10+	999	11+	11+	13+	12+	12+	12+	989	11+	11+	11+	674	x

References

1. R.M. Haralick and L.G. Shapiro, *Computer and Robot Vision*, Addison-Wesley, 1992.
2. G. Matheron, *Random Sets and Integral Geometry*, Wiley, 1975.
3. J. Serra, *Image Analysis and Mathematical Morphology*, Academic Press, 1982.
4. P. Maragos and R.W. Schafer, "Morphological system for multidimensional signal processing," *Proc. of IEEE*, vol. 78, no. 4, pp. 690-701, 1990.
5. P.A. Maragos and R.W. Schafer, "Morphological skeleton representation and coding of binary image," *IEEE Trans. Acoust. Speech Signal Process.*, vol. 34, no. 5, pp. 1228-1244, 1986.
6. P. Maragos, "Pattern spectrum and multiscale shape representation," *IEEE Trans. Pattern Analysis Mach. Intell.*, vol. 11, no. 7, pp. 701-716, 1989.
7. J. Goutsias and D. Schonfeld, "Morphological representation of discrete and binary images," *IEEE Trans. Signal Process.*, vol. 39, no. 6, pp. 1369-1379, 1991.
8. I. Pitas and A.N. Venetsanopoulos, "Morphological shape representation," *Pattern Recognition*, vol. 25, no. 6, pp. 555-565, 1992.
9. S. Loncaric and A.P. Dhawan, "A morphological signature transform for shape description," *Pattern Recognition*, vol. 26, no. 7, pp. 1029-1037, 1993.
10. E.R. Dougherty, *Digital Image Processing Methods*, Marcel Dekker, Inc. 1994.
11. F.Y. Shih and C.C. Pu, "Morphological shape description using geometric spectrum on multidimensional binary images," *Pattern Recognition*, vol. 25, no. 9, pp. 921-927, 1992.
12. C.S. Regazzoni, G.L. Foresti, and A.N. Venetsanopoulos, "Statistical pattern spectrum for binary pattern recognition," J. Serra and P. Soille(eds.), *Mathematical Morphology And Its Applications To Image Processing*, Kluwer Academic Publishers, pp. 185-192, 1994.

13. X. Zhou and B. Yuan, "Shape description and recognition using the high order morphological pattern spectrum, *Pattern Recognition*," vol. 28, no. 9, pp. 1333-1340, 1995.

Heo Jin Kim

Heo Jin Kim received the B.S. and M.S. degrees in Electronic Engineering from the Pusan Fisheries College and Ajou University, Korea., in 1983 and 1985, respectively. Since 1985 he has been with Dept. of Electronics, Dongmyung Junior College. His current research interests are in the area of digital image processing and computer vision

Gang Yi Jiang

Gang Yi Jiang was born in Zhejiang, P.R. China, in 1964. He received the B.S. and M.S. degrees in Electronics Engineering from Zhejiang Radio and Television University and Hangzhou University in 1985 and 1992, respectively. Since 1992, he has been with Hangzhou University as an associate Professor. In 1995-96, he stayed at Ajou University as a visiting Professor. His current research interests are in the area of digital image and computer vision.

Tae Young Choi

Tae Young Choi received the B. S. and M.S. degrees in Electronics Engineering from the Seoul National University, Seoul, Korea, in 1974 and 1978, respectively, and D.E.A. and Docteur-Ingênieur degrees from University of Aix-Marseille III, Marseille, France, in 1980 and 1982, respectively. In 1983, he joined the Ajou University as an assistant Professor, where he is now a Professor and Director of Academy of University-Industry Cooperation. His main interests are in the area of digital image processing and he is currently doing research on mathematical morphology and its applications.